

Paleoseismological Trenching across the Atalanti Fault (Central Greece): Evidence for the Ancestors of the 1894 Earthquake during the Middle Ages and Roman Times

by D. Pantosti, P. M. De Martini, D. Papanastassiou, F. Lemeille,
N. Palyvos,* and G. Stavrakakis

Abstract The Atalanti fault bounds to the southwest the Evoikos Gulf, one of the major extensional basins of central Greece. This fault ruptured during the 1894 earthquakes, producing at the surface a complex, ca. 30-km-long rupture. Paleoseismological trenching performed at three sites along this fault provided the first insights on its seismogenic behavior. Unfavorable trench stratigraphy and scarcity of datable material made the identification and characterization of individual paleoearthquakes quite difficult. However, by integrating paleoseismological, geological, historical, and archaeoseismological data, we defined three surface-faulting earthquakes. The most recent event is the 1894 earthquake; the penultimate occurred during the Middle Ages between A.D. 770 and 1160, whereas the third event back occurred in Roman times between 50 B.C. and A.D. 230 and is interpreted to be the Opus earthquake of A.D. 105. These results suggest that 1894-type earthquakes repeat each 660–1120 yr. The average minimum slip per event and vertical slip rates are of the order of 45 cm and 0.4–1.6 mm/yr, respectively. These values are in agreement with other geological estimates and with geodetic measurements. Because of the short time elapsed since the 1894 earthquake, the Atalanti fault does not appear to contain an important seismogenic potential. On the other hand, these results may shed light on the potential of other seismogenic sources threatening the area.

Introduction

The region of Lokris in central Greece (Fig. 1) was struck by two large shocks that occurred a week apart, on 20 April and 27 April 1894, and were followed by numerous aftershocks. According to contemporaneous reports and recent reanalyses (Mitsopoulos, 1894, 1895; Skouphos, 1894; Ambraseys and Jackson, 1990; Makropoulos and Kouskouna, 1994; Papazachos and Papazachou, 1997; Albin, 2000), the first shock was smaller. Magnitudes estimated from felt reports were between 6.4 and 6.7 for the first shock and 6.9 and 7.2 for the second (Ambraseys and Jackson, 1990; Makropoulos and Kouskouna, 1994; Papazachos and Papazachou, 1997). Macroseismic locations suggest that the first shock was located in the area of the Malessina Peninsula and the second close to the town of Atalanti (Fig. 1C).

Ground ruptures, landslides, and major disturbances of the landscape were described by contemporary authors (Davison, 1894; Mitsopoulos, 1894, 1895; Papavassiliou, 1894a,b; Philippson, 1894; Skouphos, 1894). Although the

1894 event represents one of the best examples of well-documented historical coseismic ground ruptures in the Mediterranean area, some questions are still a matter of debate, in particular those regarding which fault is responsible for the two events (IGME, 1989; Ganas, 1997; Ganas and Buck, 1998; Ganas *et al.*, 1998; Cundy *et al.*, 2000; Pantosti *et al.*, 2001). According to the contemporary reports, the first shock appears to have produced small ruptures, cracks, and landslides mainly in the Malessina Peninsula and along the coast (i.e., mostly liquefaction effects). These effects were described by Skouphos (1894) as being secondary with respect to those produced by the second shock, which seriously perturbed a coastal area exceeding 60 km in length (between the town of Agios Kostantinos and Cape Gatzia) (Fig. 1B). Most of the ruptures from the second shock appear systematically arranged along or very close to the Atalanti fault, with exceptions such as liquefaction effects along the coastal area, a landslide in Skenderaga (now Megaplatanos), some ruptures near Moulkia, and discontinuous ruptures between Atalanti and Agios Kostantinos (Fig. 1). In order to attempt a reconstruction and characterization of the 1894

*Present address: Istituto Nazionale di Geofisica e Vulcanologia, Sezione Sismologia e Tettonofisica, Roma, Italy.

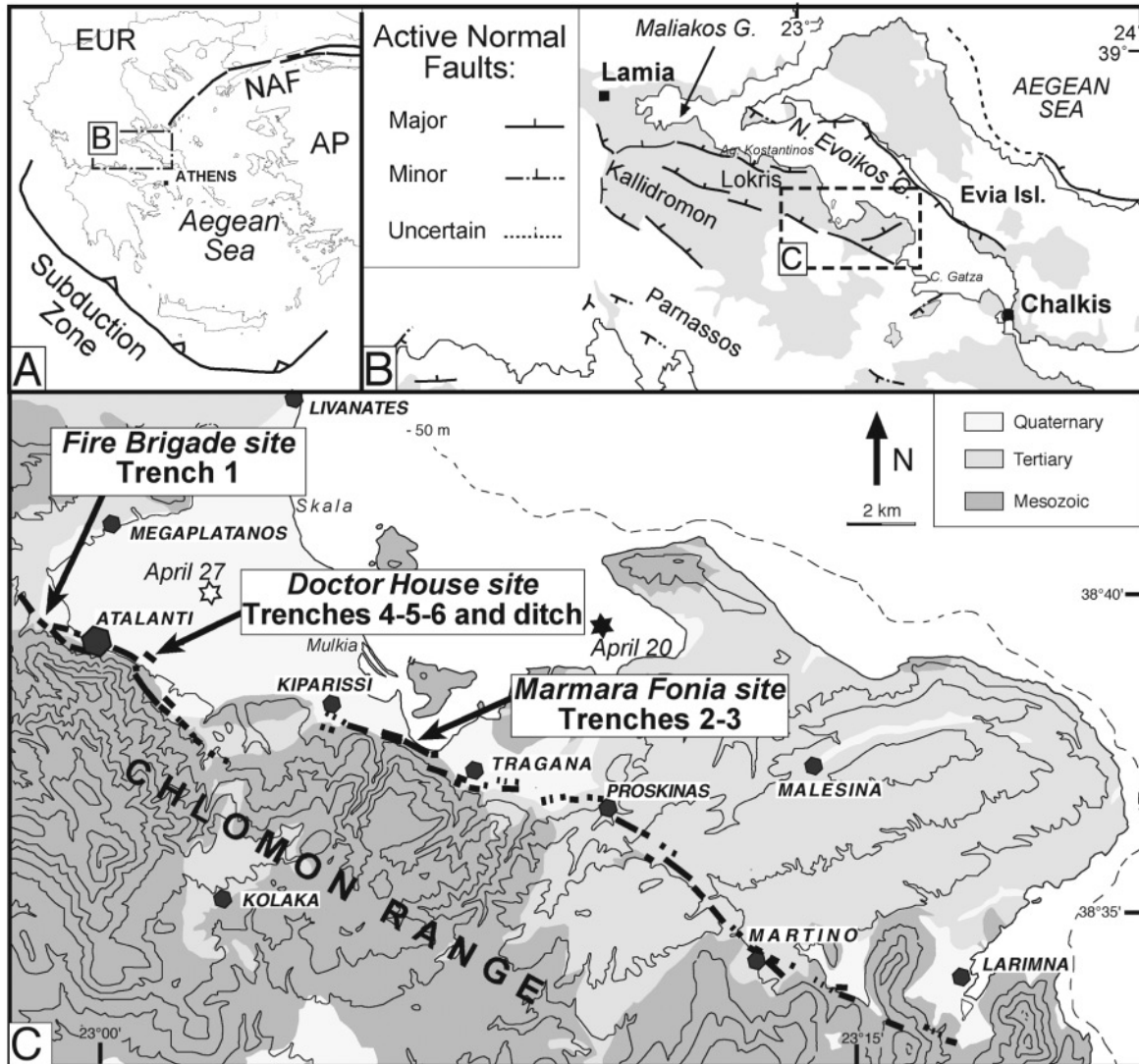


Figure 1. (A) location of study area in Greece (AP, Anatolian plate; EUR, Eurasian Plate; NAF, North Anatolian Fault). (B) Location of study area; main faults from Roberts and Jackson (1991). (C) Location of the paleoseismological trenching sites along the Atalanti fault (heavy line) as mapped in Pantosti *et al.* (2001). Macroseismic locations of the two 1894 shocks are shown with stars (after Ambraseys and Jackson [1990]).

seismogenic sources, Pantosti *et al.* (2001) used these contemporary reports coupled with investigations performed in the 1970s by Lemeille (1977) and a new aerial photo and field survey. In their reappraisal, they concluded that the first shock may have ruptured the Malessina fault or alternatively an Atalanti-parallel fault located just offshore the Malessina Peninsula, whereas the second shock ruptured the whole Atalanti fault between the towns of Atalanti and Larymna (Fig. 1C). Only the ruptures along the Atalanti fault are considered clear evidence of surface faulting (for a complete discussion, refer to Pantosti *et al.* [2001]).

Notwithstanding the debate on the 1894 sources, there is a general agreement in considering the Atalanti fault as the main active tectonic feature in the area. The fault trace

can be well recognized in the geomorphology between the towns of Atalanti and Larymna (Rondogianni, 1984; Ganas, 1997; Palyvos, 2001; Pantosti *et al.*, 2001), where it appears as a typical normal fault, bounding the Chlomon Range to the northeast (Fig. 1). The Atalanti fault forms the contact between Alpine bedrock in the footwall and Neogene or Quaternary units in the hanging wall and bounds to the southwest one of the main extensional grabens of central Greece, the North Evoikos Gulf. According to Philip (1974), this graben is subsiding at a rate of about 1 mm/yr. A recent Global Positioning System (GPS) survey suggests about 0.6–0.7 mm/yr of extension over the past century (Clarke *et al.*, 1998).

A critical question for the assessment of the seismic

hazard of this region, which appears to be threatened by other scarcely known potential seismogenic structures, is the definition of the seismic behavior of the 1894 source. The understanding of this fault may, in fact, be used as a valuable first-hand reference for the area and for the behavior of other sources. Following this aim, we started a paleoseismological trenching project on the Atalanti fault, the results of which are presented in this article.

Trenching the Atalanti Fault

At several locations, the main geomorphic trace of the Atalanti fault is paralleled within a few tens or hundreds of meters by one or more compound scarps displacing Late Pleistocene and Holocene deposits (Fig. 2). These scarps represent splays from the main fault. In most cases, these splays have a synthetic geometry with respect to the main fault and distribute the deformation at the surface over a wide zone. The 1894 coseismic ruptures occurred also along these scarps, as suggested by Pantosti *et al.* (2001) and by Figure 3. These compound scarps contain a great potential for paleoseismological trenching. In fact, because fault splay location at the surface is known within a few tens of meters and the deformed sediments are unconsolidated and recent in age (Holocene), multiple splays can be very useful for the recognition of individual paleoearthquakes. On the other hand, the existence of multiple splays in a wide zone of deformation decreases the probability of finding a complete record of faulting and consequently observing the total displacement in a trench of a reasonable length. Consequently, the possibility that some deformation (i.e., both in terms of slip amount and of number of individual events) may have occurred off the trenched scarp, and thus is missed in the trenches, should be considered. In this context, the slip estimates given herein should be considered as minimum figures.

Because of the high level of human modification for agricultural purposes, several of these scarps have been retreated and bulldozed, and at present, they are used as field boundaries or trails or are included in orchards and deeply plowed fields. Under these conditions, the geologic records (both as structures and deposits) of earthquakes of the past (especially those of 1894) can be missed and/or disrupted.

Keeping in mind these limitations, we selected several sites favorable for paleoseismological trenching along the Atalanti fault, and we excavated three of them where permission was obtained and the potential for results was higher. Two of these sites are located in the western section of the fault and one in the central section (Fig. 2). No favorable trench sites were found in the eastern section of the fault.

The sites excavated in the western section are located west and east of the town of Atalanti and referred to as the “Fire Brigade” site and the “Doctor House” site, respectively. The third site is located along the central Atalanti fault

section east of Kiparissi and is referred to as the “Marmara Fonia” site (Figs. 1 and 2).

In each trench we adopted a nomenclature for faults, stratigraphic units, samples and paleoearthquakes starting with the identification number of the trench. This is done to facilitate the reading of the text and figures and particularly to allow correlation among trenches.

The sequence exposed in each trench has been subdivided into main units depending on the nature of the matrix, the amount of oxidation and weathering of clasts, and the percentage and the size of pebbles and cobbles. Each unit is thus indicated by a letter following the identification number of the trench (i.e., 1d indicates unit d in trench 1); in a few cases sub-units are also introduced (i.e., sub-unit 1d2). In general, we trenched alluvial fan deposits, which are not optimal for paleoseismic interpretation. In particular, uncertainties related to difficulty in correlating layers (which were generally massive, containing large pebbles and cobbles, with a lack of thin and continuous layers to provide reliable slip measurements) and to the possibility of depositional hiatus and strong erosional phases should be considered.

The age of units is constrained on the basis of radiocarbon ages of organic material and on some archaeological dating. Radiocarbon dating was performed both with conventional and accelerator mass spectrometry (AMS) techniques at two different labs (Table 1). Measured ages have been corrected for $^{13}\text{C}/^{12}\text{C}$ changes in the laboratory as well as for $^{14}\text{C}/^{12}\text{C}$ changes in the atmosphere by using the calibration program Calib 4.3 (Stuiver *et al.*, 1998a,b) (Table 1). In the text and figures, we use the 2σ age intervals adjusted to the nearest decade.

Because charcoal fragments were very scarce and extremely small and thus may have been subjected to reworking or may have been part of a root much younger than the hosting sediment, dating of organic-rich material has been used extensively, although contamination from younger or older carbon may have occurred. Despite these uncertainties, we found relative stratigraphic consistency for most of the ages and conclude that these can provide an acceptable time frame for the trenched sedimentary sequences.

Stratigraphic and tectonic evidence for individual events of displacement (i.e., upper terminations of faults, faults showing increasing vertical displacement with depth, and the presence and stratigraphic position of colluvial wedges interpreted as scarp-derived deposits) have been used to define event horizons (i.e., the ground surface at the time of a surface-faulting paleoearthquake). In the text and figures, the event horizons are indicated by a number following the identification number of the trench (i.e., event 3-1 is the youngest event recognized in trench 3). An age range of the individual paleoearthquakes recognized at each trench is set on the basis of the available dated material (Table 1). On the basis of historical reports and geomorphology, we assume that the most recent earthquake recognized in all the trenches is that of 1894.

It is interesting to notice that in most cases, the geolog-

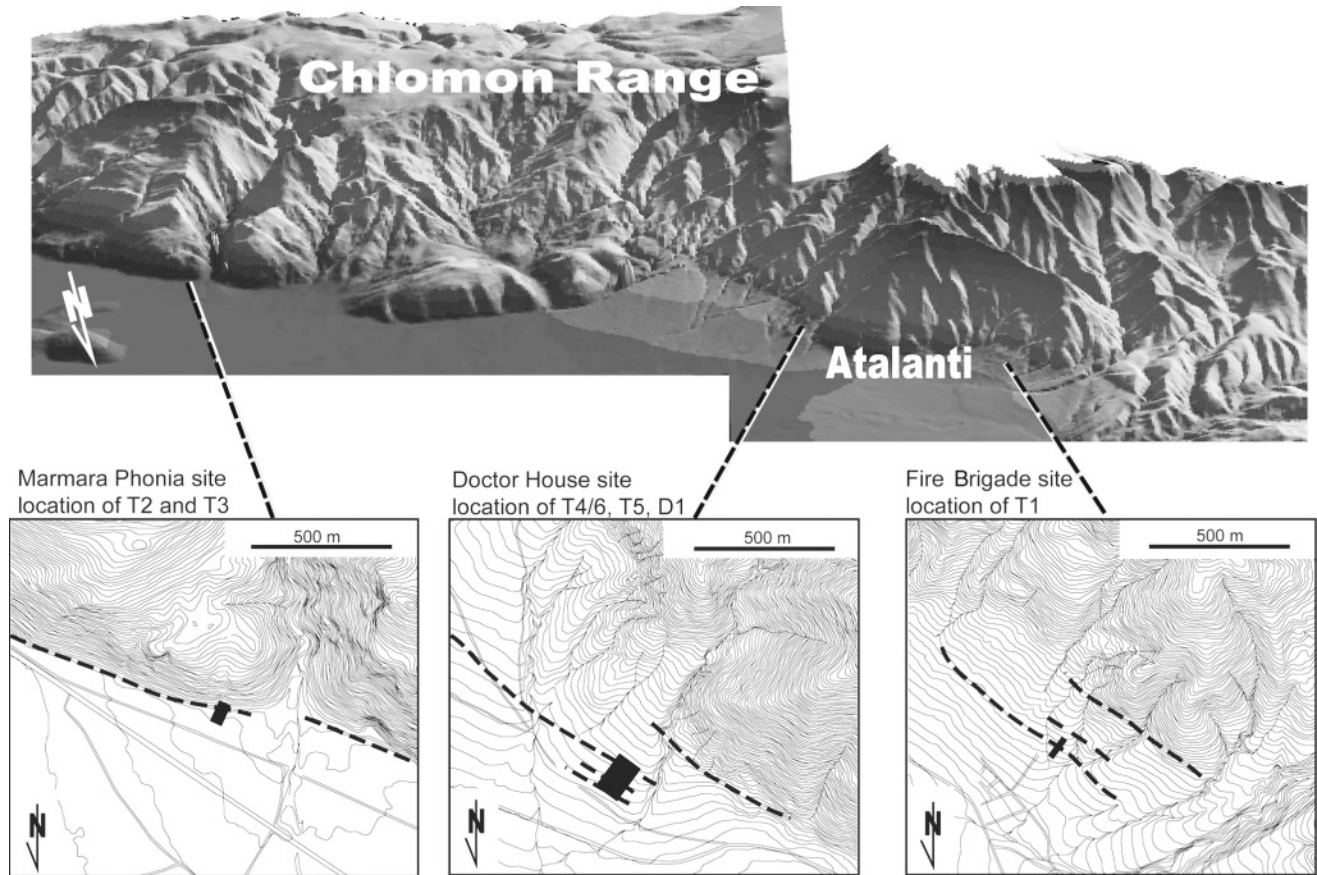


Figure 2. Top: 3D view of the central and west-northwest part of the Atalanti fault zone escarpment (vertical exaggeration 1.5) based on a 5-m Digital Elevation Model (DEM) interpolated from 4-m contours of Hellenic Army Geographical Service 1:5.000 topographic maps (Palyvos, 2001). View from N15°E, camera inclination 30°, light source from the south. Bottom: Details of trench sites. Contours are each 4 m. Dashed lines are traces of young scarps; rectangles indicate trenching sites.

ical evidence of earthquakes is obscured or deeply buried due to high rates of fan deposition; only after fan abandonment, around 3000 yr ago, when sedimentation has slowed down, is evidence of paleoearthquakes preserved.

The Trenches

The Fire Brigade Site

The Fire Brigade site is located on a coalesced, alluvial fan surface built up by relatively small seasonal creeks from the Rhoda Range, west of the town of Atalanti. Aerial photo and field surveys show evidence for two parallel, northwest-striking scarps in the alluvial fan deposits located a few hundreds of meters downslope from the main morphological escarpment (Fig. 2). The southernmost of these scarps was used to construct a wall surrounding the Fire Brigade headquarters. A 200-m-long detailed topographic profile, started at the base of this wall, shows that the northern scarp produces a vertical offset of about 1.4 m at the surface (Fig. 4A). In coincidence with this scarp, a small creek flowing

almost perpendicular to it shows a substantial decrease of the amount of incision to the north of the scarp.

Trench 1. An 18-m-long trench (T1) was excavated across the northernmost scarp, in an area where no agricultural activities appear to have occurred for many years; it was certainly abandoned before the mechanical plowing was started. The trench walls exposed a typical alluvial fan stratigraphy with some colluvium in the upper part (Fig. 4B,D). A 20- to 30-cm-thick active soil (unit 1a), with a thin humic layer at the top, is developed on a yellowish, partly cemented silty clay (unit 1b). This buries some loose organic colluvium (unit 1cw) and a compact reddish clayey silt containing small angular pebbles and a few lenses of large pebbles (unit 1d). Below this, we recognized four major alluvial units (1e, 1f, 1g, 1h) containing mainly volcanic clasts, which are distinguished on the basis of the criteria previously discussed. The upper alluvial unit 1e shows a rapid decrease of thickness northward; about half of the 1.4-m scarp detected by topographic profiling should be attributed to this nontectonic thickness change.



THE RECENT EARTHQUAKES IN GREECE: FISSURES IN THE GROUND AT ATALANTE.

Figure 3. Fissures in the ground at Atalanti, from original sketches by Bouchier (1894). Notice the multiple ruptures parallel to the main slope of the range, substantiating the findings by Pantosti *et al.* (2001) and the structures exposed in the trench walls.

Datable organic material was scarce or even totally absent in the deposits, with the exception of the upper part of the stratigraphic section, where a few charcoal fragments and organic-rich deposits are found. Also in this upper part, archaeological sherds and a brick sample of Roman or post-Roman age (1E15, maximum age 50 B.C.) has been found in unit 1cw, 30–40 cm below the surface. The ages of five samples collected in the trench (see locations in Fig. 4B) are listed in Table 1. The upper organic colluvium, unit 1cw, is consistently younger than 1000 yr B.P., confirming the archaeological findings. On the basis of a small charcoal fragment from unit 1g, which was probably reworked, the alluvial deposits have an apparent maximum age of 34 kyr (1W-02).

The zone of deformation is 6 m wide and is located below the scarp imaged with the topographic profile. This zone is formed by four major fault zones, 1F1 to 1F4 (with visible offset), together with some fractures. However, the analysis of the stratigraphy highlights that part of the imaged scarp throw is due to a sharp decrease of the thickness of one of the units exposed in the trench (unit 1e).

In this trench, we were able to discriminate three possible events of coseismic deformation. The most recent event

(1-1), that is, the 1894 earthquake, is defined because faults 1F1, 1F2, and 1F4 (where a nice open fissure formed) terminate in the active soil, almost at the present ground surface, which at this site was not plowed in the past century. Vertical throws produced by this event are hard to measure, especially because we cannot use the present ground profile for the previously mentioned reasons. No more than 22–24 cm are obtained by measuring the displacement of unit 1b across faults 1F1 and 1F2.

Three small wedges of colluvium (1cw), along with offsets of unit 1d across faults 1F1, 1F2, and 1F3, are considered evidence for the penultimate event (1-2), whose event horizon is thus located at the top of unit 1d. By using the thickness of these wedges against the faults, we can measure a rough total slip for event 1-2 of 42–45 cm.

Evidence of the third event back (1-3) is found along 1F4, where units 1h–1f are displaced about 20–25 cm, whereas the deposits above do not show any displacement but are only affected by an open fracture during the most recent event. This evidence is supported also by the observation that unit 1e shows sizeable thickening in the hanging wall of 1F4. Thus the event horizon T1-3 can be set at the base of unit 1e or possibly somewhere within it.

Table 1
List of Dated Samples

Sample*	Type	Measured Age (yr B.P.) (corrected for $^{13}\text{C}/^{12}\text{C}$)	2σ cal age years	Probability	Lab [†]
1E-16	Charcoal	230 ± 50	1516–1598 A.D.	0.138	Beta
			1617–1698 A.D.	0.347	
			1724–1814 A.D.	0.387	
			1833–1878 A.D.	0.033	
			1916–1949 A.D.	0.096	
1E-01	Charcoal	130 ± 50	1671–1779 A.D.	0.410	Beta
			1798–1945 A.D.	0.589	
1W-02	Charcoal	34060 ± 400			Beta
1E-S1	Organic sediment	540 ± 60	1299–1449 A.D.	1.00	Beta
1E-S2	Organic sediment	1090 ± 70	774–1043 A.D.	0.969	Beta
			1091–1120 A.D.	0.019	
			1140–1155 A.D.	0.012	
			1676–1763 A.D.	0.336	
2W-02	Charcoal	110 ± 40	1773–1775 A.D.	0.005	Beta
			1802–1939 A.D.	0.632	
			1946–1955 A.D.	0.027	
			3892–3675 B.C.	1.00	
2W-01	Shells	5360 ± 40			Beta
2E-S3	Organic sediment	Modern	–		Beta
2E-S2	Organic sediment	6860 ± 210	6201–6191 B.C.	0.003	Beta
			6161–6136 B.C.	0.010	
			6107–5461 B.C.	0.965	
			5450–5417 B.C.	0.012	
			4033–3845 B.C.	0.999	
3E-05	Shells	5520 ± 40	3839–3838 B.C.	0.001	Beta
			1125–1117 B.C.	0.010	
3E-S1	Organic sediment	2800 ± 60	1114–1096 B.C.	0.025	Beta
			1094–1056 B.C.	0.049	
			1055–828 B.C.	0.915	
			779–1058 A.D.	0.934	
4E-S1	Organic sediment	1070 ± 70	1087–1122 A.D.	0.042	BRGM
			1138–1156 A.D.	0.024	
			44 B.C.–233 A.D.	1.00	
4E-S2	Organic sediment	1930 ± 60			BRGM
4W-S1	Organic sediment	2230 ± 40	389–199 B.C.	0.998	Beta
			185–185 B.C.	0.002	
5W-S1	Organic sediment	1380 ± 70	534–782 A.D.	0.984	BRGM
			791–812 A.D.	0.011	
			843–855 A.D.	0.005	
5W-S3	Organic sediment	3030 ± 80	1437–1019 B.C.	1.00	BRGM
5W-30	Charcoal	1560 ± 70	345–352 A.D.	0.006	Beta
			355–369 A.D.	0.013	
			381–641 A.D.	0.981	
5E-03	Charcoal	?Modern			Beta
5W-S5	Organic sediment	2740 ± 40	995–992 B.C.	0.004	Beta
			974–954 B.C.	0.061	
			944–809 B.C.	0.935	
			690–704 A.D.	0.025	
6E-S1	Organic sediment	1210 ± 40	707–753 A.D.	0.130	BRGM
			758–897 A.D.	0.812	
			922–943 A.D.	0.033	
			694–697 A.D.	0.004	
6W-S2	Organic sediment	1190 ± 40	717–747 A.D.	0.055	BRGM
			766–903 A.D.	0.821	
			916–964 A.D.	0.119	
			975–975 A.D.	0.001	

Measured and calibrated ages (according to Calib 4.3 by Stuiver *et al.* [1998]) of the samples collected in the trenches.

*The first number of the sample indicates the trench where it was collected; E or W indicates the wall.

†Beta: dating performed by Beta Analytic Inc., Miami, Florida, USA; BRGM: dating performed by the geochronology laboratory of the Bureau de Recherches Géologiques et Minières, France.

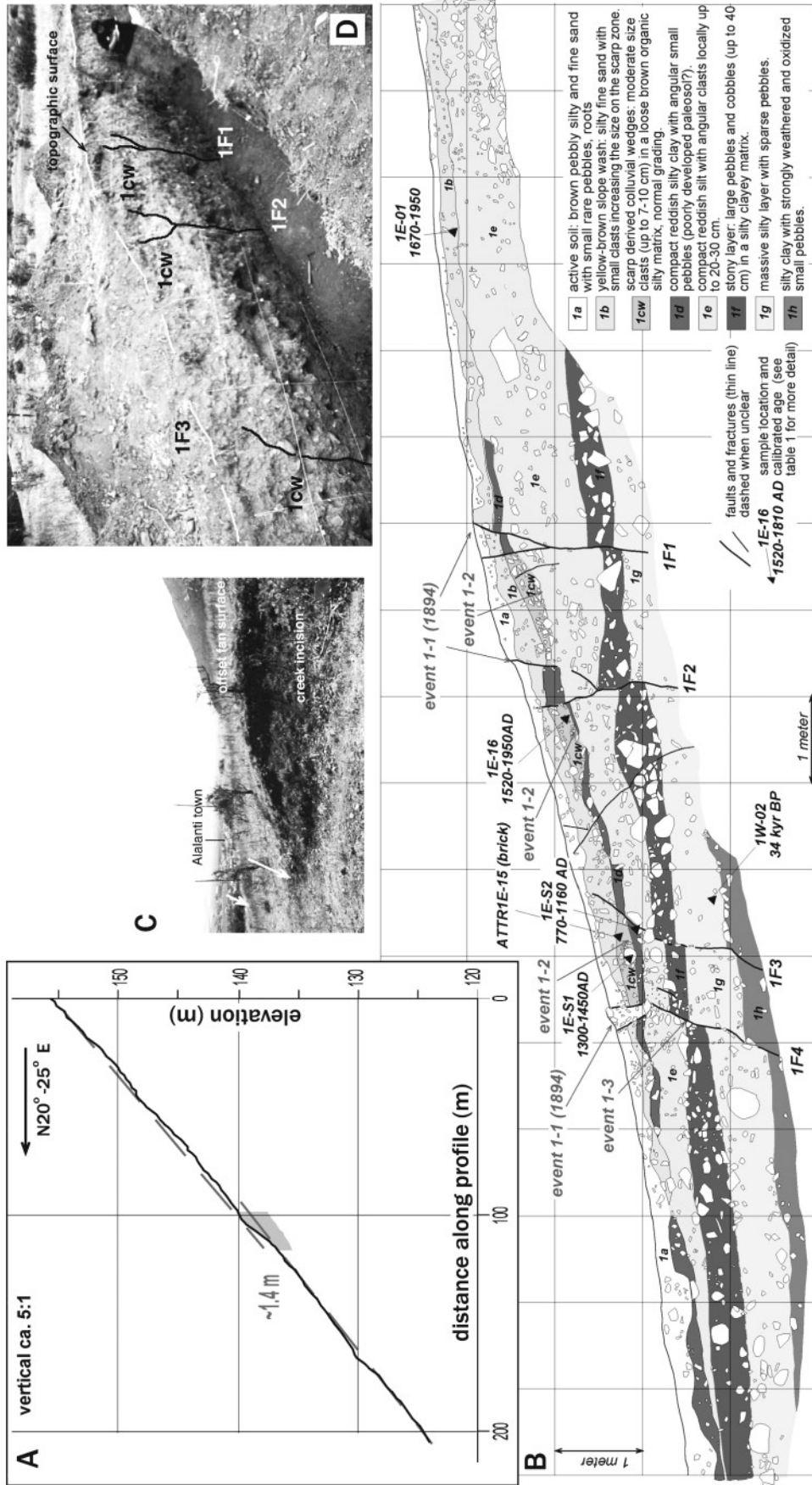


Figure 4. (A) Topographic profile across the Fire Brigade scarp with trench location (shaded area), vertical exaggeration 5. (B) Simplified log of trench 1, east wall from a 1:20 survey. (C) View of the northern scarp (white arrows) where it is dissected by a small seasonal stream. (D) Photo of the eastern wall of trench 1; grid spacing is 0.5 m vertical and 1 m horizontal.

The total displacement produced by these three events measured on the base of unit 1e is 0.6–0.7 m. Adding the individual measurement of displacement previously discussed, we obtain 0.8–0.9 m. This indicates that we are somehow overestimating the individual throws or that we are not correctly reconstructing the original geometry of unit 1e. One possibility is that because of the difficult stratigraphy, the throws based on the thickness of colluvial wedges contain some biases. Another possibility is that we are overestimating the number of events recorded in the trench. However, recognition of E1-1 and E1-3 is quite strong because the first produces the displacement of the entire sequence up to the surface and crosscuts one of the colluvial wedges interpreted as post-penultimate event deposits and the second is constrained by the offset of unit 1e. Event E1-2 is based mainly on the interpretation of post-event colluvial wedges; thus, it can be more debatable, but we do not have other explanations for the presence of the colluvium next to the fault traces other than the presence of a fault scarp. On the basis of the available data, we cannot solve this question; to be conservative, we assume a total slip for the three events of 0.6–0.7 m, which will give an average slip per event of 0.20–0.23 m.

In the assumption of the three events, on the basis of

the limited age constraints available in this trench (see Table 1), the timing of events is set as follows: event 1-2 preferred age between A.D. 770 and 1450 with the possibility of ages as young as 1950 but with lower probabilities (samples 1ES2, 1ES1, and 1E16), and event 1-3 older than A.D. 1160 (sample 1ES2).

The Doctor House Site

At the Doctor House site, multiple scarps offset a wide, gently convex alluvial fan derived from erosion of Mt. Rhoda. Most of the debris and matrix in the fan are composed of weathered volcanics. A 170-m-long detailed topographic profile shows the presence of three major scarps located about 300 m north of the range front with a total vertical offset of the fan surface ranging between 2.7 and 3.5 m (Figs. 2 and 5A,B). At this site, we opened two trenches (T4/6 and T5) and a long exploratory ditch (D1) connecting them.

Trench 4/6. The overlap of trenches 4 and 6 (15 and 9 m long, respectively) provides about 18 m of exposure across the southernmost scarp, where a 1.4-m vertical offset is measured. Overlapping trenches were excavated to avoid destruction of an intact, large vase used for food storage, as

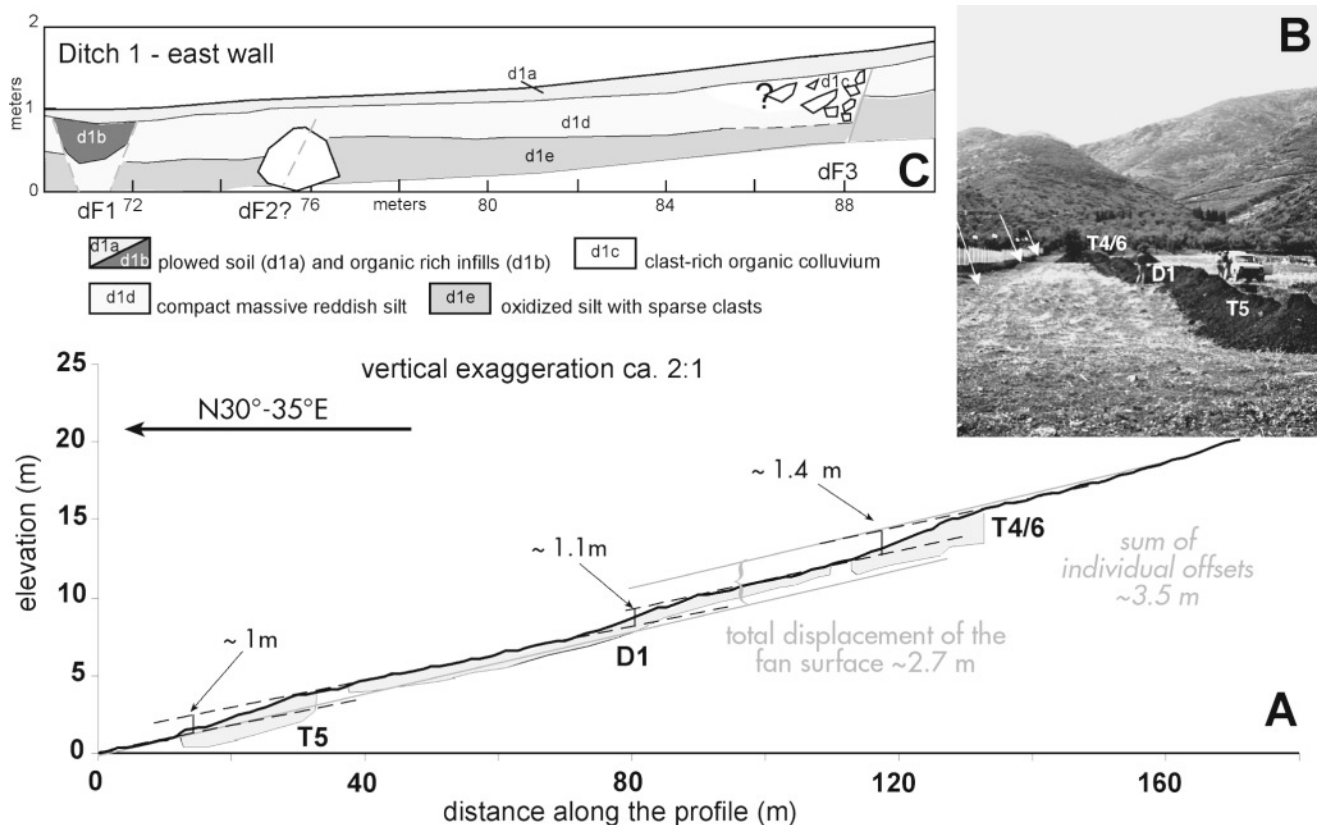


Figure 5. (A) Topographic profile across the scarps at the Doctor House site with trench and ditch relative locations (shaded area). (B) View of the site from the north. (C) Log with simplified stratigraphy of the ditch in the central scarp zone; meter ticks are the same as in (A).

old as Roman times (Fig. 6). Because we were able to correlate the two trench exposures, we treat them as a single trench (T4/6) in the discussion that follows. The trench walls expose alluvial fan deposits, mainly matrix supported, under a plowed 20- to 30-cm-thick active soil (unit 4/6a, Fig. 6). We distinguished five major alluvial and colluvial units (4/6b–4/6f) composed of rounded to angular clasts in a silty matrix. We were not able to trace a contact between 4/6c and 4/6d in trench 6, probably because of the lack of calcrete development; thus, we refer to the unit between 4/6b and 4/6e as 4/6c + d in this trench. Datable charcoal was not found in this trench, so organic-rich units were dated as bulk samples. The age of the upper colluvial units 4/6b and 4/6c is in the range 40 B.C. to A.D. 1160 (Table 1). These ages are in agreement with the archaeological estimate of the age of the Roman vase (50 B.C. to A.D. 200; Local Archaeological Office, S. Dimaki, personal comm., 1999) that was found within these units. According to dating from unit 4/6f, alluvial deposition seems to have occurred no later than a few centuries B.C.

The whole zone of deformation in this trench is about 10 m wide, consisting of four major fault zones (4/6F1–4/6F4). The Roman vase was located within fault zone 4/6F4, apparently in a man-made widening of an open fracture. On the footwall of 4/6F1, important weathering with calcrete formation produced a calcarosol (unit 4/6f) developed on the alluvium 4/6e. The calcarosol is found only on the fault footwall because it was exposed and stable for a longer time with respect to the hanging wall that was experiencing tectonic subsidence instead. The presence of this unit prevented a clear correlation of units across the fault zone.

Evidence for three surface-faulting events was found. The surface ruptures of the 1894 event (T4/6-1) have been destroyed by intense plowing. However, a subtle break in slope in the topographic profile exactly above faults 4/6F1 and 4/6F2, the upper termination of these faults just below the plowed layer, plus shearing and displacement of young deposits (unit 4/6b) is considered to be the evidence for this earthquake. Due to the modification of the ground surface and of the irregular geometry of the young layers, it is difficult to measure the vertical throw produced by the 1894 earthquake across this trench. By matching the surface profile, the gentle scarplet at 4/6F1 and 4/6F2 suggests a vertical throw not exceeding 20 cm, whereas 7–14 cm can be estimated at 4/6F4 (trench 6) by matching some secondary layering in 4/6b or the top of 4/6c, assuming all of its offset is derived from the 1894 event. More slip occurred at 4/6F3, but it cannot be distinguished by that produced by the penultimate event; as a first approximation, the 14–18 cm measured on the top of 4/6c can be tentatively equally divided on the two events.

Evidence for a penultimate event (T4/6-2) is the upper termination of faults 4/6F2 and 4/6F4 at the base of unit 4/6b and the deposition of a scarp-derived colluvium covering the whole zone of deformation (unit 4/6b). The event horizon for this event would be located at the base of 4/6b. In-

dividual vertical throws can be separated from those produced by the other events only across 4/6F1 and 4/6F2 and are between 43 and 55 cm on the basis of the thickness of 4/6b near the fault zone. For the reasons mentioned earlier, at 4/6F3 a throw of 7–9 cm can be assumed. Not much displacement seems to have occurred at 4/6F4.

Finally, a third event back (T4/6-3) was defined on the basis of an increase of displacement with depth at 4/6F4 (displacement of the base of 4/6c is ca. 60 cm, whereas that of the base of 4/6b is 12–15 cm), thickening of 4/6c + d on the hanging wall of 4/6F4, and the possible interpretation of unit 4/6c or 4/6c + d as a scarp-derived post-event deposit. That 4/6c + d could be a post-earthquake deposit is supposed on the basis of the observation that the thickness of unit 4/6c + d is strongly controlled by its location with respect to the faults, suggesting that a displacement event occurred during its deposition and possibly at the contact between 4/6d and 4/6c (where mapped). If this interpretation is correct, the event horizon would be located at the base of 4/6c. After this event there may have been an open fissure at the deformation zone 4/6F4, where the vase was found, and people may have placed there the vase full of offers to earthquake gods. Vertical throws are 22–25 cm and 16–38 cm across the two splays of 4/6F4 and 7–14 cm at 4/6F3, measured on the top of 4/6e by subtracting the displacement produced by the younger events. A throw of 18–28 cm minimum is estimated on the basis of the thickness of 4/6c against 4/6F1, following the assumption that this is a scarp-derived deposit.

By using available ages and recognized event horizons, the timing of paleoearthquakes recorded in this trench is set as follows: event T4/6-2 between 40 B.C. and A.D. 1160 (samples 4ES2 and 4ES1), and T4/6-3 between A.D. 230 (sample 4ES2) and 50 B.C. in the hypothesis of the emplacement of the Roman vase just after this event.

Trench 5. A 21-m-long trench (trench 5, T5) was opened across the northernmost scarp, where a 1.0-m vertical offset is measured at the surface (Fig. 5A). Similarly to trench 4/6, this trench also exposes alluvial fan deposits (Fig. 7), mainly matrix supported. Under a plowed active soil (unit 5a), we distinguished three colluvial (5a1, 5b1, 5b2) and two major alluvial (5c and 5d) units composed of rounded to angular clasts in a silty matrix; a calcarosol-type unit (5e) appears to have developed on unit 5c on the footwall of 5F3. The upper part of the alluvial units contain rare and small clasts with respect to the lower ones; the matrix is generally finer and prevailing with respect to the deposits of T4/6, in agreement with a more distal position of trench 5 in the fan. Also in this trench, important weathering on the footwall of the major fault zones 5F3 and 5F4 make hard the correlation of units across them. A few small charcoal samples and bulk soils were collected for dating. The few datable ones indicate that the colluvial units 5b and 5c were deposited after 1440 B.C. and that the calcarosol 5e is about 3000 yr old (sample 5W-S5; Table 1), indicating that no fan deposition occurred

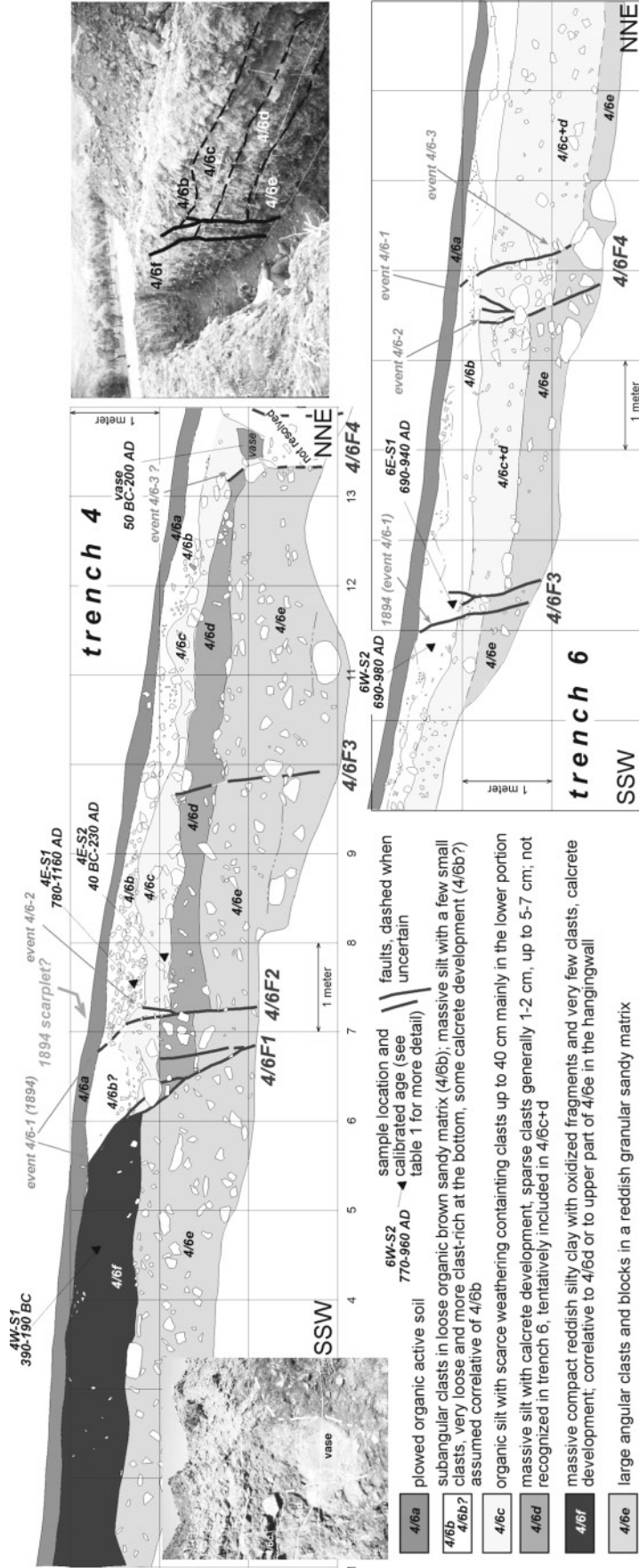


Figure 6. Simplified logs of the west walls of trenches 4 and 6. The trench relative elevation and overlap in figure are based on field measurements. Logs are reduced from a 1:20 survey. The photos show a view of the western wall of trench 4 (upper right) with a grid spacing of 0.5 m vertical and 1 m horizontal and the vase found at 13–14 m in trench 1 (left).

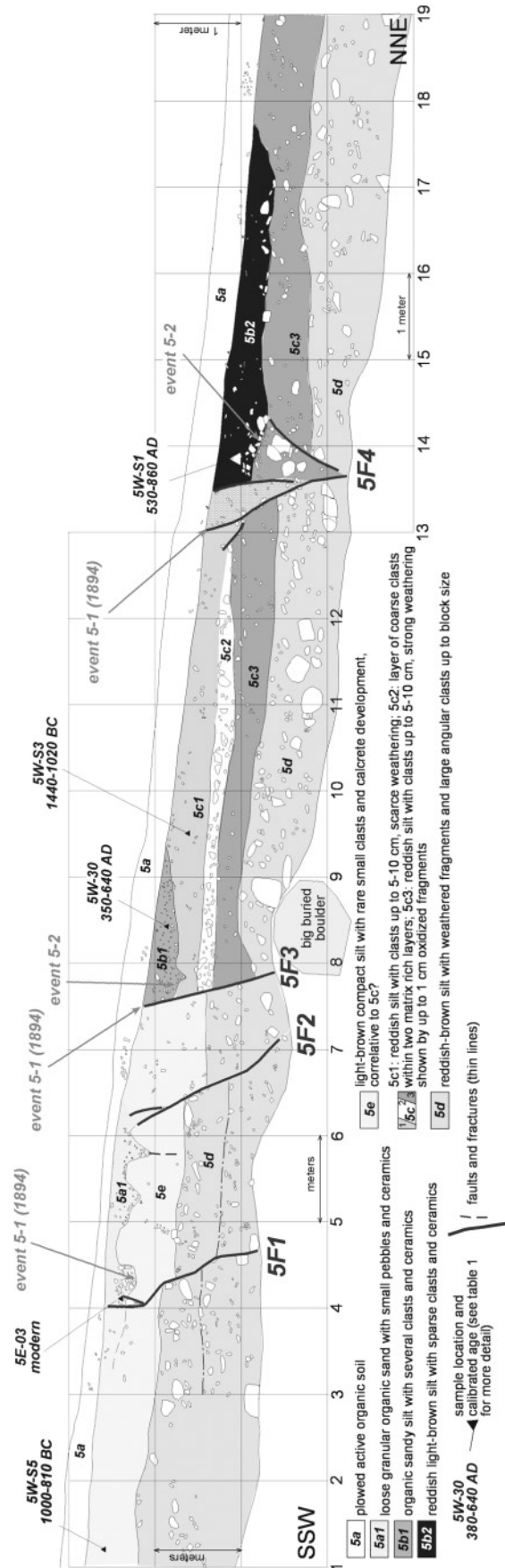


Figure 7. Simplified log of trench 5, west wall, from a 1:20 survey.

at least during the past ca. 3000 yr, in agreement with the observations in T4/6.

The zone of deformation is about 10 m wide and is formed by four major fault zones (5F1 to 5F4). The style of deformation is very similar to that of T4/6, with slip distributed along several splays.

Only two events of coseismic deformation could be defined here. Evidence for the surface rupture of the 1894 earthquake is the shearing of the entire sequence (e.g., at 5F4) up to the base of the plowed layer along with some open cracks with infilling of recent material (at fault zone 5F1). Although the ground surface is highly modified by human activities, some subtle evidence of the 1894 scarps can be found in the steepening of the ground surface (Fig. 7). A 47- to 50-cm vertical throw for the 1894 earthquake can be estimated by reconstructing the ground profile, but it is difficult to be measured as offset of layers because it is combined with that produced by the penultimate event. The penultimate event (event T5-2) is recognized because of the upper termination of faults (at fault zone 5F4) as well as development of scarp-derived colluvial wedges (5b1 and 5b2). Because we do not have relations that constrain unequivocally the formation of these post-earthquake scarp-derived units, we cannot rule out the possibility that they were formed during two subsequent paleoearthquakes. Vertical displacements can be estimated on the basis of the thickness against the 5F3 and 5F4 fault zones of the two scarp-derived deposits (5b1 and 5b2), which are 35–37 and 43–45 cm, respectively. These should be added if we assume they formed because of the same earthquake or treated independently if they are the result of two individual events. Also, by measuring the total vertical displacement recorded by the top of unit 5d, and assuming this is offset only produced by the two events recognized, we obtain a throw of 120–162 cm. By subtracting from this the 47- to 50-cm throw attributed to the 1894 event, a total throw of 70–98 cm is obtained. This is in agreement with the estimates based on the thickness of the scarp-derived colluvium. The limited age constraints available indicate that the event(s) 5-2 occurred between A.D. 860 (sample 5W-S1) and 1440 B.C. (sample 5W-S3), likely closer to the younger part of this interval.

Ditch 1. An 80-m-long, 1-m-deep, narrow exploratory ditch was opened across the central scarp and was extended to reach the end of the other trenches (Fig. 5). The aim of this shallow excavation was to perform a rapid survey to establish a possible correlation between the stratigraphy exposed in the two trenches and to explore the central scarp.

The agricultural layer, 20 to 30 cm thick, is covering the whole exposure. Along the ditch we recognized the typical fan deposits similar to those located in the fault footwalls exposed in both trenches: a very compact, massive, fine-grained layer rich in calcrete (calcarosol?), overlying an oxidized silty layer with sparse subangular clasts up to 10 cm. At some locations the upper massive layer thins out, disap-

pears completely, or is interrupted by clast-rich colluvium.

Both ditch walls show three main lateral anomalies in geometry, color, and lithology, which could be interpreted as fault zones. These anomalies are located at meters 70, 76, and 88, respectively, and coincide at the surface with the change in slope forming the central scarp (Fig. 5A,C).

The 71-m anomaly appears as a sharp depression, filled with an organic-rich deposit, interrupting the stratigraphy. If this is not a large burrow, it may be evidence of an open fissure produced by the 1894 earthquake or by a previous seismic event. At 76 m there is a step in the stratigraphy, but the presence of a large boulder prevented the identification of the nature of this discontinuity. At 88 m the anomaly is very clear, and a sharp stratigraphic contrast suggests the occurrence of a fault bringing in contact a fan sequence (agricultural layer, massive fine layer, and stony oxidized layer at the bottom) with colluvium. If this colluvium is interpreted as a scarp-derived deposit, this is evidence for the occurrence of a paleoearthquake very comparable with what was found in the other excavations.

No unique correlation can be deduced on the basis of the ditch interpretation. One possibility is that the so-called fan sequence, with the massive, fine calcrete-rich layer on top, represents the final stage of fan deposition on which a calcarosol started to develop (approx. close to the age of samples 4W-S1 and 5E-S5, ca. 2000–3000 yr B.P.), whereas all the deposits that are found in the hanging wall of the fault zones are a consequence of surface faulting. As already mentioned, this would also explain why evidence of paleoearthquakes is found only in the upper part of the trench stratigraphy. In fact, because of the high energies and rates of sedimentation, an active fan environment would not allow for preservation of coseismic features.

The Marmara Fonia Site

At the Marmara Fonia site, the scarp is located in slope deposits at the base of a steep limestone front, a typical setting for a normal fault (Fig. 2). Although severe human modification has taken place at this site for the construction of an electricity line and for agricultural purposes, a 70-m-long detailed topographic profile shows the presence of a scarp with vertical offset of about 0.8 m at the surface (see Pantosti *et al.*, 2001).

Trench 2. A 14-m-long trench (T2) was opened, exposing mainly scree and slope-derived deposits composed of angular clasts up to boulder size, in a silty reddish matrix (Fig. 8). The size of clasts and matrix generally decreases downslope. Under a thin active soil layer (unit 2a), three main units (2b, 2d, 2f) and two small fine silty wedge-shaped colluvial deposits of local origin (2c, 2e) can be distinguished. In the middle part of the trench, a big boulder, which fell down from the steep slope to the south (there are several boulders still at the surface that, according to Skouphos [1894], fell from the slope during the 1894 earthquakes), interrupts the stratigraphy and is buried by younger deposits.

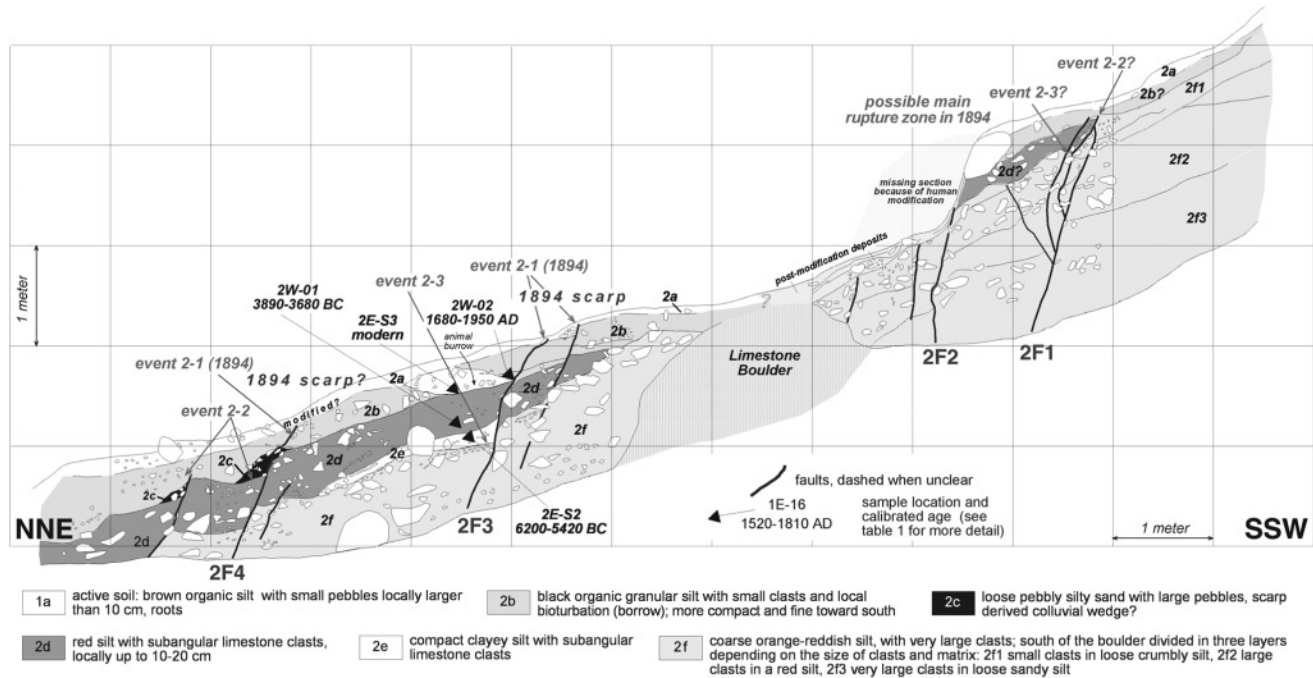


Figure 8. Simplified log of trench 2, east wall, from a 1:20 survey.

A correlation of units at both sides of the boulder is attempted.

Datable organic material was very rare; some bulk soils were sampled, as were some marine shells (probably food taken by humans from the sea nearby) and charcoal fragments. Because of the setting of the site and of the type of sediments exposed in the trench, important reworking and inclusion of old carbon in young deposits may have occurred. If this is the case, the ages that were obtained should be considered as the maximum possible age for the deposit. The ages of four of the samples collected in the trench walls are listed in Table 1. The oldest sample collected in the section was taken from unit 2e and gave an apparent maximum age of 6200 B.C.

The zone of deformation is 9 m wide and can be divided, with respect to the big boulder, into a northern and southern section. In the latter, we recognized two major fault zones (2F1, 2F2); the lack of datable material, together with intense human activity that caused the artificial retreat of the scarp, makes the interpretation of this part of the trench very difficult, and thus it remains ambiguous. In the northern section, two more fault zones (2F3, 2F4) are located.

Evidence for the 1894 earthquake, that is the most recent event (event 2-1), is found at faults 2F3 and 2F4, which terminate in the active soil and correspond to two scarp-sets on the surface profile, and possibly at 2F2. Because of the human modification of the site, displacement on 2F2 cannot be measured; thus only a minimum vertical displacement for this event can be estimated. Assuming the scarps at the surface are entirely produced by the 1894 earthquake, ca. 15 cm and 13–25 cm of vertical displacement are measured at

2F4 and 2F3, respectively. A penultimate event (event 2-2) can be inferred on the basis of offset of unit 2d across fault zone 2F4 and 2F1 and of small scarp-derived colluvial wedges (units 2c) deposited against 2F4 that appear as a distinct wedge-shaped accumulation of normally graded coarse material, which seem to fill completely the throw of the faulted sequence. The event horizon is set in the northern part of the trench at the top of unit 2d. Vertical throws for this event are 17–27 cm at the two splays of 2F4. An older event can be located at fault 2F3, at the top of unit 2f. This is defined because of the larger offset of unit 2f compared to the units above it and due to the presence of a wedge-shaped colluvium (unit 2e) against the fault. A vertical throw of 25–27 cm can be measured. Further displacement of 27–34 cm is recognized at 2F1; its attribution to one of the events discussed earlier is problematic. Unit 2d? against fault 2F1 could be interpreted as a scarp-derived deposit or as the remnant of a faulted colluvial unit. In the first case, the displacement will be associated to event 2-2; otherwise it would be evidence of event 2-3. Because of this unsolvable ambiguity, we assume this slip to be produced by both events, and we split it in two contributions of ca. 15 cm each for the slip calculation.

Based on the available datings, timing of paleoearthquakes prior to the 1894 earthquake is set as follows: penultimate event T2-2 could be anytime between 3890 B.C. and the present (samples 2-W01 and 2-W02), event T2-3 should be older than 3680 B.C. (sample 2W-01).

Trench 3. A 15-m-long trench (T3) was opened 50 m west of T2 at a location where the scarp appeared to be less mod-

ified. Due to the dense vegetation cover, we had to locate the trench in a lower slope position with respect to T2. Similarly to T2, trench T3 exposes mainly scree and slope-derived stratigraphy (Fig. 9) quite difficult to decipher. Under a thin active soil layer (unit 3a), we distinguished six main colluvial units (3b–3g). These units are composed of angular clasts in a silty reddish matrix; we were not able to correlate unequivocally these units with those exposed in T2, except for the lower unit 3f that appears to be correlative of 2f on the basis of their characteristic granular orange matrix. A set of wedge-shaped scarp-derived colluvial deposits (units 3h1, 3h2, and 3h3) is developed in the main fault zone at the base of the slope.

Very limited datable material was found; what could be sampled was some marine shells like those in trench 2 and organic soils to constrain mainly the ages of the youngest colluvium close to the main fault zone. Ages in the range 4030–830 B.C. were found (Table 1). The upper layers to

the north contain several pottery fragments, indicating they are younger than 2000–3000 yr old.

The zone of deformation is 5 m wide and located at the southern end of the section, where four faults were mapped (3F1–3F4). The main fault zone consists of faults 3F1 and 3F2 and is characterized by severe shearing and imbrication of clasts. Stratigraphic units cannot be confidently traced through it.

Evidence for the 1894 earthquake (event 3-1) is found at fault 3F2, where faulting reaches the surface and has induced the development of an incipient colluvial wedge (3h1). A further indication is the small offset observed along the southern branch of fault 3F4, along with the presence of a small loose deposit (3h1) on top of unit 3b, which is interpreted as scarp-derived colluvium. A penultimate surface-faulting paleoearthquake (event 3-2) can be inferred by the fact that the northern branch of fault 3F2 has its upper termination at the base of unit 3h2, which is a wedge of col-

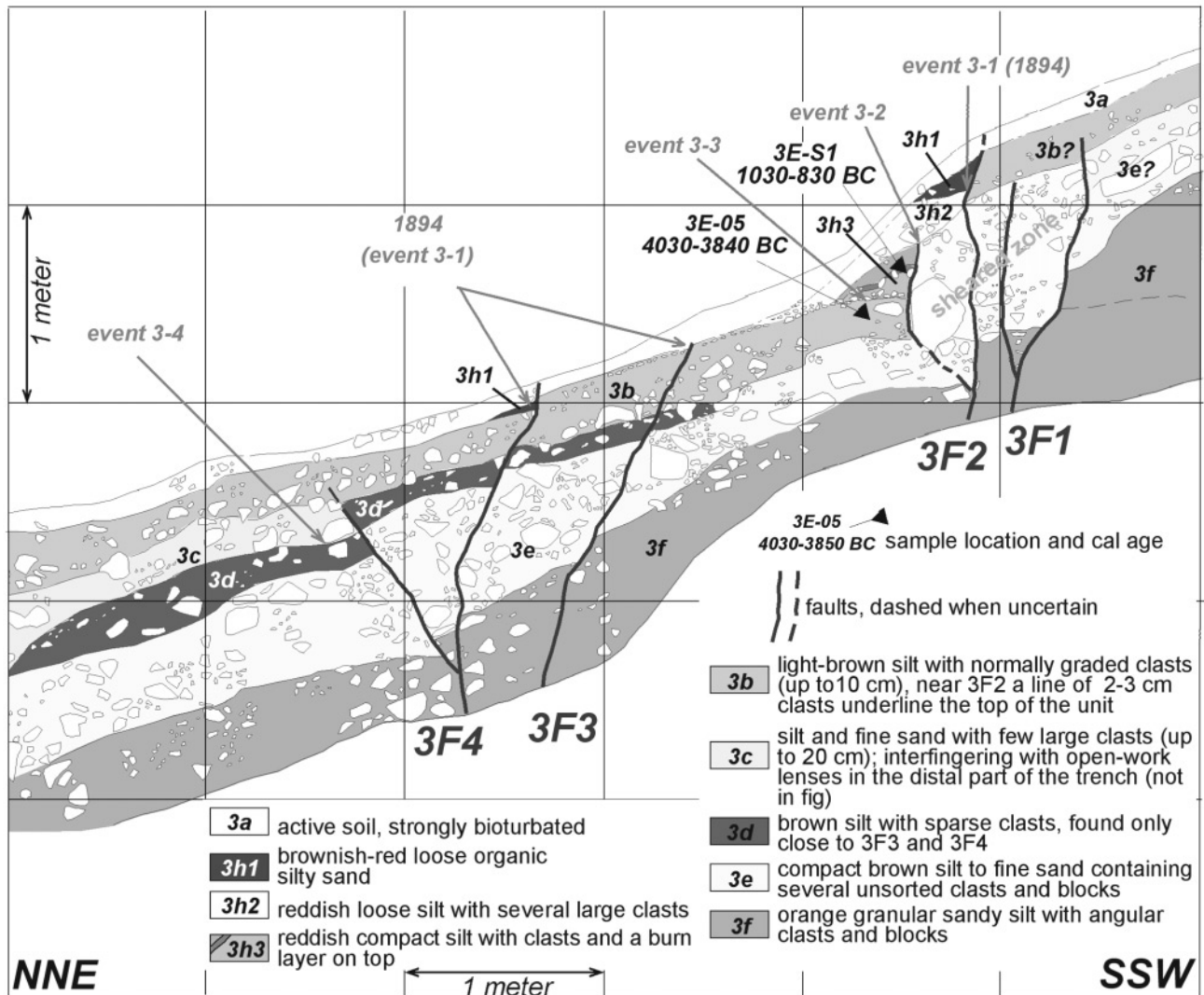


Figure 9. Simplified log of the southern portion of trench 3, east wall, from a 1:20 survey.

luvium deposited after surface faulting occurred. An older event (3-3) is defined due to the development of an older colluvial wedge (unit 3h3) on top of unit 3b. Evidence for a further event back in time (3-4) is found at the northern branch of fault 3F4, where the lower units 3d to 3f show an apparent reverse offset of 20 cm, whereas unit 3b appears crossed only by fracturing. Coseismic vertical throws are difficult to measure. The use of colluvial wedges for event recognition and estimation of slip per event is highly debatable, but because this was the only way to obtain slip estimates in this trench, it was nevertheless attempted, and a consistent figure ranging between 22 and 26 cm for all the events is found. These values have to be considered as minima, because some of the deformation zone may have been lost since the trench may have intercepted only the northern zone of deformation seen in T2.

Constraints on the ages of these events are very limited and ambiguous, especially if possible inclusion of old carbon in younger deposits is considered as discussed for trench T2. The penultimate event (3-2) should be younger than 1130 B.C. (sample 3E-S1), the third event back (event 3-3) is bracketed between 4030 B.C. (sample 3E-05) and 830 B.C. (sample 3E-S1), whereas event 3-4 should be older than 3840 B.C. (sample 3E-05).

Pre-1894 Surface-Faulting Earthquakes on the Atalanti Fault

Paleoseismological Evidence of Past Earthquakes

The paleoseismological investigations at the three different trench sites (Figs. 1 and 2) along the Atalanti fault provided evidence for repeated surface-faulting events prior to 1894. The correlation of paleoearthquakes recognized at different sites remains a matter of debate in paleoseismology. In fact, dating constraints, even if of good quality, are not enough to correlate with certainty the coseismic geological evidence found at different sites with the same earthquake. Moreover, which part of the fault ruptured, the whole fault or at least the part between the two sites?

According to Pantosti *et al.* (2001), the 27 April 1894 shock ruptured the entire Atalanti fault; however, the fault shows some intrinsic complexity related to pre-existing transverse structures. On the basis of fault geometry and geomorphology, Pantosti *et al.* divided the Atalanti fault into three sections: western, central, and eastern. Two of the studied sites (Fire Brigade and Doctor House) are located in the western section, while the third one (Marmara Fonia) is located in the central section. No sites favorable for trenching were found in the eastern section.

Even with these uncertainties, assuming that the 1894 rupture extent is typical of the Atalanti fault and that its internal complexity is not too strong to allow shorter ruptures, we may attempt to correlate events by using their relative stratigraphic position and their chronological constraints

(Fig. 10). It should be noticed that because of the weakness of the chronological constraints, different correlations are possible. In the following, we present the simplest correlation we could find.

As already mentioned, we assume that the most recent event recognized in each trench is the 1894 earthquake; this on the basis of the historical reports, and it is supported by the observation that the ruptures still visible in the trenches are very close to the surface or terminate just below the plowed topsoil.

For the previous events, we tried to merge information from all sites. However, the ages obtained from trenches 2 and 3 at the Marmara Fonia site are significantly older than the others, introducing a further element of uncertainty. This may suggest on the one hand that the central part of the fault has a different rupture history than the western part with exception for the 1894 earthquake, or on the other that there is contamination from older carbon at this site or important hiatuses of deposition. Because of this, the dating from the Marmara Fonia site is not used to place critical age constraints.

The penultimate event was constrained between A.D. 770 and 1450 (possibly 1950) in T1, between 50 B.C. and A.D. 1160 in T4/6, and between 1440 B.C. and A.D. 860 in T5 (Fig. 10). If we consider the overlap of the first two intervals, we may infer that the penultimate event on the Atalanti fault (hereafter ATL-PEN) occurred between A.D. 770 and 1160. An older event was found in the trenches (hereafter ATL-OLD) that is older than A.D. 1160 in T1 and occurred between 50 B.C. and A.D. 230 in T4/6 and between 940 B.C. and A.D. 640 in T5. All these ages overlap, and the best age estimate we can get for ATL-OLD is between 50 B.C. and A.D. 230. Event T5-2 can be either ATL-PEN or ATL-OLD, as age overlap exists with both. Even though the age overlap is smaller, because the stratigraphic position of event horizon 5-2 is consistent with that of 4/6-2, in the following we assume as a first hypothesis that event 5-2 is ATL-PEN. Ages of events 2-2 and 3-2 are compatible with both intervals of time and do not add any further constraint. The ages of old events in T2 and T3 may suggest evidence for a previous event older than 3000 yr.

Historical, Archaeological, and Geological Evidence of Past Earthquakes

The 1894 earthquake was extensively described by contemporary authors and reappraised in more recent works (for a detailed description, see Pantosti *et al.* [2001]). Thus, no more discussion will be devoted here to this event. Information on previous earthquakes is quite scarce, but there are historical reports or archaeological and geological evidence for destruction likely produced by earthquakes in the broader Atalanti fault area.

The oldest indication of a destructive earthquake is archaeological evidence of the destruction of storage buildings at the archaeological site of Kynos (Dakoronia, 1996) near Livanates (Fig. 1C). The archaeological dating places this



Figure 10. Summary of the ages of paleoearthquakes recognized in the trenches opened along the Atalanti fault and comparison with historical events. A tentative correlation of events between trenches is proposed on the basis of their relative stratigraphic position and absolute dating. Black bars are age intervals of radiocarbon samples used for constraining the paleoearthquakes (only the used samples are reported). Thick gray bars indicate age ranges of events at different sites (arrows are used when one of the range boundaries is not constrained); different tones of gray for the bars are used to indicate events we correlated. Thick vertical lines locate historical events. Shaded areas indicate the best estimate age interval of the surface faulting events pre-dating 1894. Because of the weakness of the age constraints from the Marmara Fonia site, they were not used to constrain ages of events. Event ATL-PEN does not have any correlative historical event, whereas ATL-OLD is in all likelihood the A.D. 105 Opus earthquake. In the upper left inset, paleoseismological vertical throw measurements described in the text are shown as thick bars, white portions indicating the throw ranges. MF, Marmara Fonia site (based on estimates from T1); DH, Doctor House site (based on estimates from T4/6 + T5); FB, Fire Brigade site (based on estimates from T2).

possible seismic destruction at around 1100 B.C., a period that is in agreement with the dating of a possible event of rapid coastal subsidence by Pirazzoli *et al.* (1999). Dating marine bioerosion marks, they proposed an event of up to 0.9 m of rapid (coseismic) subsidence between 1380 and 965 B.C. (Pirazzoli *et al.*, 1999). The association of this subsidence event to an earthquake at the Atalanti fault is problematic, because Kynos may be located on the hanging wall of the Atalanti fault (thus it is expected to undergo coseismic subsidence due to its activity), but simple dislocation models (see Figure 13 in Pantosti *et al.* [2001] for details) show that for 1 m of slip on the Atalanti fault, no more than 10 cm of subsidence are expected at Kynos. This, along with the fact that Pirazzoli *et al.* (1999) also inferred another event at Kynos but of important uplift this time, together with the existence of several active faults in the area, make the definitive attribution of these events to a specific fault a difficult task.

The best known historic earthquake that struck the North Evoikos region is that of the summer of 426 B.C., an earthquake whose dramatic impact was described by Thucydides, Diodore the Sicilian, and Strabo. Ganas (1997), Ganas *et al.* (1998), and Stiros and Pirazzoli (1995) associated this event with the Atalanti fault, but historical reports suggest that it should have originated much to the northwest, in the Maliakos Gulf (Fig. 1B) (Bousquet and Pechoux, 1977; Makropoulos and Kouskouna, 1994; Ambraseys and White, 1997; Papazachos and Papazachou, 1997).

Another event, which has not attracted much attention in the past, occurred in A.D. 105. Eusebios of Pamfile, Paulos Orossios, and George Syngellos inform us that a strong earthquake destroyed Atalanti (Opus) and Orei (in the island of Evia) during the eighth year of the reign of the Roman emperor Trajan (Guidoboni *et al.*, 1994; Papazachos and Papazachou, 1997). Archaeological evidence of large destruction during this period is found both in the Atalanti area

and along the coast, near Skala (Local Archaeological Office, S. Dimaki, personal comm., 1999), as well as in a location very close to Kynos (Livanates) where Gaki-Papanastassiou *et al.* (2001) radiocarbon dated a possible seismic destruction event at 150 ± 90 calendar yr A.D. (destruction layer with extensive remains of fire).

Finally, according to Evangelatou-Notara (1993), on the basis of Venetian historical documents, another historical earthquake occurred in the area of central Evia, in A.D. 1417 (Vite de' Duchi di Venezia, edit. L.A. Muratorius, R.I.S., 22, Milano 1733). The historical reports mention a very strong event. Niemi (1990), after sedimentological research in the southern shore of the Maliakos Gulf about 30 km northwest of Atalanti, where archaeological ruins are exposed during low tide, revealed evidence for a seismic event that subsided the area in ca. A.D. 1400. Although there is no other evidence to relate the A.D. 1417. earthquake with this subsidence event, their age consistency and location of subsidence suggests that the A.D. 1417 earthquake probably did not occur on the Atalanti fault but rather on one of the faults located farther northwest.

By comparing paleoseismological and historical events, we can summarize our findings as follows (Fig. 10):

1. Evidence for the 1894 earthquake is found in all trenches.
2. ATL-PEN occurred in the interval A.D. 770–1160 and does not have any known correlative event in the historical record.
3. ATL-OLD occurred in the interval 50 B.C.–A.D. 230 and may well be the A.D. 105 Opus earthquake.

These results support the hypothesis (Ambraseys and White, 1997) that the 426 B.C. earthquake did not occur on the Atalanti fault.

Size of the Ancestors of the 1894 Earthquake

The size of the surface faulting produced by the three earthquakes recognized in the trenches (1894, ATL-PEN, and ATL-OLD) could be compared both on the basis of the rupture length and of the slip per event observed at each site. There are not enough data available to discuss the size of the earthquakes on the basis of extent of surface faulting. We can only state that on the basis of correlation of events, ATL-PEN appears to have ruptured at least the central and western sections of the Atalanti fault.

Limited information about coseismic vertical displacement exists. As already discussed, because of the peculiarity of the rupture, that is, splaying near the surface in different branches (Fig. 3), the vertical slip evaluations should be generally considered as minima. In fact, depending on which splay(s) took most of the slip during an event and whether this was exposed or not in our excavations, these estimates may change substantially. Vertical throws measured at the different fault zones are added up in each trench. Moreover, the throws derived from the different trenches at the Doctor

House site should be added due to the presence of the three parallel scarps. Not knowing the timing of faulting at the central scarp, we cannot provide a complete evaluation of the throws at each fault splay.

Starting from the westernmost trench site, vertical throws are estimated as in the following and shown in the inset of Figure 10: 1894 event, 20–23 cm in T1, 34–43 cm in T4/6 that should be added to 47–50 cm from T5, 28–40 cm from T2, and 22–26 cm from T3; ATL-PEN, 20–23 cm in T1, 50–64 cm in T4/6 that should be added to 70–98 from T5 in the assumption this is from one single event, 32–42 cm in T2, and 22–26 cm in T3; ATL-OLD, 20–23 cm from T1, 45–77 cm from T4/6, 40–42 cm from T2, and 22–26 cm in T3.

Even considering all the uncertainties already discussed related to the possible partial exposure in the trenches of the coseismic deformation, from this summary (inset in Fig. 10) it is clear that the largest total throws per event, even exceeding 1 m, are observed at the Doctor House site. The possibility that the large throws obtained for ATL-PEN at this site may be the result of the inclusion of some throw related to ATL-OLD that we were not able to distinguish in T5 should be considered. Even with these uncertainties, an average value of ca. 45 cm can be obtained for the three sites with averages of ca. 22, 96, and 38 cm at the Fire Brigade, Doctor House, Marmara Fonia sites, respectively. Comparing these paleoseismological values with those retrieved from the 1894 contemporary descriptions (for a detailed discussion, see Pantosti *et al.* [2001]) reporting in general 100 cm of vertical offset, with ranges between 30 and 200 cm, a good agreement is observed. Pantosti *et al.* (2001) suggested that the wide range of observations of coseismic throws for the 1894 earthquake is strongly related to the peculiarity of the rupture, which reached the surface as several splays (Fig. 3) running both at the contact between bedrock and scree/alluvium or within soft Quaternary deposits. This appears to be likely for the paleoseismological estimates too.

In summary, considering that: (1) the paleoseismological vertical throws observed at the three sites should generally be considered minimum values, and all exceeded a few tens of centimeters to reach up to more than 1 m (inset in Fig. 10); (2) there is a strong similarity of throw values retrieved from the paleoseismological trenches and those in the contemporary 1894 earthquake reports; (3) at least ATL-PEN ruptured two sections of the Atalanti fault; and (4) according to the empirical relations proposed by Wells and Coppersmith (1994), the observed paleoseismological vertical throws are compatible with a surface rupture length ranging between 28 and 32 km (from average displacement versus surface fault length and maximum displacement versus surface fault length for normal faults); we conclude that the ancestors of the 1894 earthquake had a similar magnitude (ca. M 6.8 according to Pantosti *et al.* [2001]), compatible with rupture of the whole Atalanti fault.

Conclusions

Paleoseismological trenching at three sites along the Atalanti fault provided information about the age of the two surface-faulting earthquakes that occurred prior to the 27 April 1894 shock, which apparently ruptured the entire fault. Although with uncertainty and leaving open possible alternative interpretations, the penultimate event ATL-PEN occurred during the Middle Ages, between A.D. 770 and 1160, whereas the previous event ATL-OLD occurred during the Roman Age, between 50 B.C. and A.D. 230, and is interpreted to be the A.D. 105 Opus earthquake mentioned in historical accounts. No evidence for the famous 426 B.C. earthquake was found. These ages suggest the occurrence of a large surface-faulting earthquake on the Atalanti fault every 660–1120 yr. The vertical offset observed in the trenches should be considered generally a minimum, and it ranges between 0.2 and 1.9 m with a 45-cm average for each paleoearthquake. These values are consistent with those reported in 1894 by contemporary authors. This similarity with the 1894 rupture size along with the empirical relations proposed by Wells and Coppersmith (1994) suggests that the 27 April 1894 earthquake is a typical earthquake for the Atalanti fault. No new constraints for the extent of the surface rupture were found. The vertical slip rate for the Atalanti fault was suggested by Ganas (1997) and Ganas *et al.* (1998) to range between 0.27 and 0.4 mm/yr and by Pantosti *et al.* (2001) to range between 0.1 and 0.5 mm/yr during the Late Pleistocene and between 0.2 and 1.2 mm/yr during the Holocene. Trench data provide new information to attempt two different estimates of vertical slip rate by using (1) the average slip per event (45 cm) and the recurrence interval (660–1120 yr), which would indicate a 0.4–0.7 mm/yr vertical slip rate, or (2) the age of the fan surface at the Doctor House site, obtained from dating in the trenches (samples 4W-S1 and 5W-S5) and its offset across the three scarps (2.7–3.5 m assuming it was regularly developed with no mimicking from earlier events), which indicate a vertical slip rate of 0.9–1.6 mm/yr.

Assuming an average dip of 60° for the Atalanti fault, vertical slip rates of 0.4–1.6 mm/yr would roughly translate to an extension rate of 0.2–0.9 mm/yr. Considering all the uncertainties associated, these estimates are in good agreement with the 1-mm/yr subsidence proposed by Philip (1974) and with the 0.6- to 0.7-mm/yr GPS extension rate across the Evoikos Gulf from Clarke *et al.* (1998).

Acknowledgments

We are indebted to H. Maroukian, K. Gaki-Papanastassiou, G. D'Addezio, and L. McNeill for their support and discussion in the field, to the mayor of the town of Atalanti, to the staff of the local archaeological office, and in particular to Mrs. F. Dakoronia and S. Dimaki for their precious cooperation. We would like to thank also two anonymous reviewers whose comments and suggestions helped substantially improve the paper. The European Community project FAUST (ENV4-CT97-0528) funded most of this work, with additional funding from the Istituto Nazionale di Geofisica e Vulcanologia and the National Observatory of Athens.

References

- Albini, P. (2000). Una rilettura dei forti terremoti del 20 e 27 Aprile 1894 nella Locride (Grecia centrale), in *G.N.G.T.S. XIX National Congress Extended Abstracts Volume*, 7–9 November, Roma (in Italian), 190–191.
- Ambraseys, N. N., and J. A. Jackson (1990). Seismicity and associated strain of central Greece between 1890 and 1988, *Geophys. J. Int.* **101**, no. 3, 663–708.
- Ambraseys, N. N., and D. White (1997). The seismicity of the eastern Mediterranean region 550–1 B.C.: a reappraisal, *J. Earthquake Eng.* **1**, 603–632.
- Bourchier, W. C. (1894). Sketches for the *Illustrated London News*, 2 June, vol. 54, no. 2876, p. 692.
- Bousquet, B., and P.Y. Pechoux (1977). La séismicité du bassin Egeen pendant l'Antiquité: méthodologie et premiers resultats, *Bull. de la Soc. Géol. de France* **19**, no. 3, 679–684.
- Clarke, P. J., R. R. Davies, P. C. England, B. Parsons, H. Billiris, D. Paradissis, G. Veis, P. A. Cross, P. H. Denys, V. Ashkenazi, R. Bingley, H.-G. Kahle, M.-V. Muller, and P. Briole (1998). Crustal strain in central Greece from repeated GPS measurements in the interval 1989–1997, *Geophys. J. Int.* **135**, 195–214.
- Cundy, A. B., S. Kortekaas, T. Dewez, I. S. Stewart, I. W. Croudace, H. Maroukian, D. Papanastassiou, K. Gaki-Papanastassiou, K. Pavlopoulos, and A. Dawson (2000). Coastal impacts of the 1894 Gulf of Atalanti earthquakes, central Greece, *Marine Geology Spec. Publ.* **170**, 3–26.
- Dakoronia, Ph. (1996). Earthquakes of the Late Helladic III period (12th century B.C.) at Kynos (Livanates, central Greece), in *Archaeoseismology*, British School of Archaeology at Athens, Fitch Laboratory Occasional Paper 7, 41–44.
- Davison, C. (1894). M. Papavasiliore on the Greek earthquakes of April 1894, *Nature* **1303**, no. 50, 607.
- Evangelatou-Notara, F. (1993). Earthquakes in Byzantium from the 13th to the 15th century; historical examination, *Parousia* **24**, 179 pp., Athens (in Greek).
- Gaki-Papanastassiou, K., H. Maroukian, D. Papanastassiou, N. Palyvos, and F. Lemeille (2001). Geomorphological study in the Lokrian coast of N. Evoikos Gulf (central Greece) and evidence of palaeoseismic destructions, in *36th CIESM Congress*, Monaco, September, 25.
- Ganas, A. (1997). Fault segmentation and seismic hazard assessment in the Gulf of Evia rift, central Greece, *Ph.D. Thesis*, University of Reading, United Kingdom, 368 pp.
- Ganas, A., and V. A. Buck (1998). A model for the tectonic subsidence of the Allai archaeological site, Lokris, central Greece, *Bull. Geol. Soc. Greece* **32**, no. 1, 181–187.
- Ganas, A., G. P. Roberts, and T. Memou (1998). Segment boundaries, the 1894 ruptures and strain patterns along the Atalanti fault, central Greece, *J. Geodyn.* **26**, no. 2–4, 461–486.
- Guidoboni, E., A. Comastri, and G. Traina (1994). *Catalogue of Ancient Earthquakes in the Mediterranean Area up to the 10th Century*, Istituto Nazionale di Geofisica, Rome, 504 pp.
- Institute of Geology and Mineral Exploration (IGME) (1989). Seismotectonic map of Greece, scale 1:500,000, IGME, Athens.
- Lemeille, F. (1977). Etudes néotectoniques en Grèce centrale nord-orientale (Eubée centrale, Attique, Béotie, Locride) et dans les Sporades du Nord (île de Skiros), in *Thèse de Troisième Cycle*, Université Paris XI, Centre Orsay, 173 pp. (in French).
- Makropoulos, K. C., and V. Kouskouina (1994). The 1894 April 20 and 27 Atalanti earthquakes: 100 years after—lessons learnt, in *Proc. and Activity Report of the 1992–94 XXIV European Seismological Commission*, Vol. 1, 61–71, 19–24 September, Athens, Greece.
- Mitsopoulos, K. (1894). Die Erdbeben von Theben und Lokris in der Jahren 1893 und 1894, *Abdruck aus Dr. A. Petermanns Geogr. Mitteilungen* **10**, 1–11 (in German).
- Mitsopoulos, K. (1895). *The Mega-Earthquake of Lokris in April 1894*, Ethnikon Typografeion, Athens, 40 pp. (in Greek).

- Niemi, T. (1990) Paleoenvironmental history of submerged ruins on the northern Euboan gulf coastal plain, central Greece, *Geoarchaeology* **5**, no. 4, 323–347.
- Palyvos, N. (2001). Geomorphological study of the broader Atalanti area, *Ph.D. Thesis*, University of Athens, 234 pp. (in Greek).
- Pantosti D., P. M. De Martini, D. Papanastassiou, N. Palyvos, F. Lemeille, and G. Stavrakakis (2001). A reappraisal of the 1894 Atalanti earthquake surface ruptures, central Greece, *Bull. Seism. Soc. Am.* **91**, 760–780.
- Papavassiliou, A. (1894a). Sur le tremblement de terre de Locride (Grèce) du mois d' avril 1894, *C. R. Acad. Sci. Paris* **19**, 112–114 (in French).
- Papavassiliou, A. (1894b). Sur la nature de la grande crevasse produite à la suite du dernier tremblement de terre de Locride, *C. R. Acad. Sci. Paris* **19**, 380–381 (in French).
- Papazachos, B. C., and C. B. Papazachou (1997). *The Earthquakes of Greece*, P. Ziti, Thessaloniki, Greece, 159–304 (in Greek).
- Philip, H. (1974). Etude néotectonique des rivages égéens en Locride et en Eubée nord-occidentale (Grèce), in *Thèse de Troisième Cycle*, Académie de Montpellier, Université des Sciences et Techniques du Languedoc, 103 pp. (in French).
- Philippson, A. (1894). Das dies jährige Erbeben in Lokris, *Zeitschrift Ges. Erdkunde zu Berlin* **21**, 332–334 (in German).
- Pirazzoli, P., S. Stiros, M. Arnold, J. Laborel, and F. Laborel-Deguen (1999). Late Holocene coseismic vertical displacements and Tsunami deposits near Kynos, Gulf of Euboa, central Greece, *Phys. Chem. Earth* **24**, no. 4, 361–367.
- Roberts, S., and J. Jackson (1991). Active normal faulting in central Greece: an overview, in *The Geometry of Normal Faults*, A. M. Roberts, G. Yielding, and B. Freeman (Editors), Geological Society Sp. Publ. 56, 125–142.
- Rondogianni, Th. (1984). Etude neotectonique des rivages occidentaux du canal d'Atalanti (Grèce centrale), in *Thèse de Troisième Cycle*, Univ. Paris XI, 190 pp. (in French).
- Skouphos, T. (1894). Die swei grossen Erdbeben in Lokris am 8/20 und 15/27 April 1894, *Zeitschrift Ges. Erdkunde zu Berlin* **24**, 409–474 (in German).
- Stiros, S. C., and P. A. Pirazzoli. (1995). Palaeoseismic studies in Greece: a review, *Quatern. Int.* **25**, 57–63.
- Stuiver, M., P. J. Reimer, E. Bard, J. W. Beck, G. S. Burr, K. A. Hughen, B. Kromer, F. G. McCormac, J. van der Plicht, and M. Spurk (1998a). INTCAL98 Radiocarbon age calibration 24,000–0 cal BP, *Radiocarbon* **40**, 1041–1083.
- Stuiver, M., P. J. Reimer, and T. F. Braziunas (1998b). High-precision radiocarbon age calibration for terrestrial and marine samples, *Radiocarbon* **40**, 1127–1151.
- Wells, D. L., and K. J. Coppersmith (1994). New empirical relationships among magnitude, rupture length, rupture width, rupture area, and surface displacement, *Bull. Seism. Soc. Am.* **84**, 974–1002.
- Istituto Nazionale di Geofisica e Vulcanologia
Sezione Sismologia e Tettonofisica
Via di Vigna Murata 605
I-00143 Roma, Italy
pantosti@ingv.it
(D. Pantosti, D.M.D.)
- National Observatory of Athens
Institute of Geodynamics
P.O. Box 20048 Gr-11810
Athens, Greece
(D. Papanastassiou, G.S.)
- Institute de Radioprotection et Sureté Nucleaire
BB17 F-92265
Fontenay aux Roses, France
(F.L.)
- University of Athens
Department of Geology
Panepistimiopolis Zografou, 15784
Athens, Greece
(N.P.)